1α,25-Dihydroxyvitamin D_3 Modulation of Adipocyte Reactive Oxygen Species Production

Xiaocun Sun and Michael B. Zemel

Abstract

SUN, XIAOCUN AND MICHAEL B. ZEMEL. 1α,25-Dihydroxyvitamin D_3 modulation of adipocyte reactive oxygen species production. *Obesity.* 2007;15:1944–1953.

Objective: We have previously shown 1α,25-dihydroxyvitamin D_3 [1α,25-$(OH)_2D_3$] to inhibit mitochondrial uncoupling protein 2 (UCP2) expression in adipocytes and that in vivo suppression of calcitriol levels with calcium-rich diets increases UCP2 expression. Because UCP2 plays a significant role in the clearance of reactive oxygen species (ROS), we studied the effect of calcitriol on ROS production and ROS-induced adipocyte proliferation.

Research Methods and Procedures: ROS production in human and murine adipocytes was stimulated by high glucose (30 mM) or H_2O_2 (100 nM).

Results: Both approaches resulted in increased ROS production by 27% to 100% ($p < 0.05$) and increased cell proliferation by 15% to 39% ($p < 0.03$). These effects were augmented by the addition of mitochondrial uncoupling inhibitor guanosine 5′-diphosphate (GDP; 100 μM) or 1α,25-$(OH)_2D_3$ (10 nM) and attenuated by UCP2 overexpression, suggesting that inhibition of mitochondrial uncoupling suppresses clearance of ROS and increases adipocyte proliferation. The addition of $\alpha \pm$ tocopherol (1 μM) inhibited cell proliferation in adipocytes treated with either H_2O_2 or high glucose, indicating that ROS plays a major role in the regulation of cell proliferation in adipocytes. Moreover, stimulation of ROS with high glucose and H_2O_2 resulted in a 2- to 5-fold increase in adipocyte intracellular calcium ($[Ca^{2+}]i$; $p < 0.001$), and calcium channel antagonism (nifedipine, 10 μM) suppressed ROS induced calcium influx and cell proliferation, indicating that $[Ca^{2+}]i$ may also regulate ROS production and exert a mitogenic effect in adipocytes.

Discussion: These data support a role of 1α,25-$(OH)_2D_3$, UCP2, and $[Ca^{2+}]i$ in the regulation of adipocyte ROS production.

Key words: calcitriol, calcium, reactive oxygen species, uncoupling protein 2

Introduction

An increase in fat mass in obesity may result from recruitment of new adipocytes (1,2), an increase in the volume of existing adipocytes (3), and/or attenuation of apoptosis (4–6). Thus, the adipogenic potential of precursor cells may be an important determinant in fat mass regulation and obesity-associated disorders. However, increased adiposity is also an adaptive mechanism for an organism in response to increased energy intake, because it provides an alternative for ectopic accumulation of lipid into liver, skeletal muscle, and pancreatic β cells (7,8). Indeed, lipodystrophy in humans and mice leads to excess ectopic triglyceride storage and severe insulin resistance and diabetes (9–11). Although adipogenesis may function to an extent as an adaptive mechanism activated during caloric excess, the mechanisms of regulation of adipocyte proliferation are not yet clear.

The production of reactive oxygen species (ROS)[1] has been shown to be increased in obesity and diabetes (12,13). It has been postulated that hyperglycemia and hyperlipidemia, key clinical manifestations of obesity and diabetes, may promote ROS production through various pathways (14). Indeed, the generation of ROS as byproducts of the mitochondrial electron transport chain has long been attributed to the high rates of glucose and lipid metabolism. Furthermore, additional mechanisms may be operated to

Received for review March 6, 2006.
Accepted in final form January 18, 2007.
The costs of publication of this article were defrayed, in part, by the payment of page charges. This article must, therefore, be hereby marked "advertisement" in accordance with 18 U.S.C. Section 1734 solely to indicate this fact.
Department of Nutrition, University of Tennessee, Knoxville, Tennessee.
Address correspondence to Michael B. Zemel, Department of Nutrition, University of Tennessee, 1215 West Cumberland Avenue, #229, Knoxville, TN 37996-1900.
E-mail: mzemel@utk.edu

[1] Nonstandard abbreviations: ROS, reactive oxygen species; $[Ca^{2+}]i$, intracellular calcium; NADPH, nicotinamide adenine dinucleotide phosphate; UCP, uncoupling protein; 1α,25-$(OH)D_3$, 1α,25-dihydroxyvitamin D_3; DMEM, Dulbecco's modified Eagle's medium; RT-PCR, reverse transcriptase-polymerase chain reaction; GDP, guanosine 5′-diphosphate; SE, standard error; NF-κB, nuclear factor-κB.

produce ROS under high glucose and high lipid conditions, including the formation of advanced glycation end products (15), and altered polyol pathway activity (16), activation of oxidases (17,18), and/or reduction of antioxidant enzymes (19,20).

Although ROS may adversely affect cell survival because of membrane damage and irreversible DNA modification (21), ROS also may function as specific signaling molecules involved in cell proliferation and growth (22). Early experiments showed low concentration of superoxide or hydrogen peroxide (10 nM to 1 mM) to be effective in stimulating the in vitro proliferation and growth response in a variety of cultured mammalian cell types (23–27). Although the molecular mechanism of the regulation of cell growth and proliferation by ROS is not yet clear, several mechanisms have been proposed. First, ROS can modulate expression of early growth-related genes, leading to aberrant expansion of rapidly growing clones and to tumor formation (28). Second, ROS may contribute to growth factor transduction pathways through alterations in protein-tyrosine phosphorylation mediated by both protein tyrosine kinase and protein tyrosine phosphatase activities (29). Third, a group of nuclear transcription factors are modulated by redox status, and ROS can activate these molecules by causing their release from their inactive cytoplasmic complex (30).

The regulation ROS production and interactions among ROS, calcium, and mitochondrial uncoupling have been intensively studied. Calcium signaling is essential for production of ROS and elevated intracellular calcium ($[Ca^{2+}]i$) activates ROS-generating enzymes, such as nicotinamide adenine dinucleotide phosphate (NADPH) oxidase and myeloperoxidase, and formation of free radicals by the mitochondrial respiratory chain (31). Interestingly, increased ROS production also stimulates $[Ca^{2+}]i$ by activating calcium channels on plasma membrane and endoplasmic reticulum (32). Thus, ROS may modulate calcium-dependent physiologic processes, whereas manipulation of calcium signaling may also regulate cellular ROS production. Respiration is associated with production of ROS, and mitochondria can produce a large portion of total cellular ROS (33). Mild uncoupling of respiration diminishes mitochondrial ROS formation by dissipating the mitochondrial proton gradient and potential (34). Accordingly, mild activation of mitochondrial uncoupling protein (UCP) may play a role in the antioxidant defense system.

Previous studies from this laboratory have shown an anti-obesity effect of dietary calcium, with increasing dietary calcium inhibiting lipogenesis, stimulating energy metabolism, and increasing adipocyte apoptosis (35). These effects are mediated by suppression of 1α,25-dihydroxyvitamin D_3 [1α,25-$(OH)_2D_3$], which stimulates Ca^{2+} influx through a non-genomic effect (36) and suppresses mitochondrial *UCP2* gene expression (37). Because ROS production is modulated by mitochondrial uncoupling status and $[Ca^{2+}]i$ homeostasis, both of which can be regulated by 1α,25-$(OH)_2D_3$, we studied the effects of 1α,25-$(OH)_2D_3$ on ROS production and ROS-induced cell proliferation.

Research Methods and Procedures

Cell Culture

3T3-L1 preadipocytes were incubated at a density of 8000 cells/cm^2 (10-cm^2 dish) and grown in Dulbecco's modified Eagle's medium (DMEM) containing 10% fetal bovine serum and antibiotics (adipocyte medium) at 37 °C in 5% CO_2 in air. Confluent preadipocytes were induced to differentiate with a standard differentiation medium consisting of DMEM-F10 (1:1, vol/vol) medium supplemented with 10% fetal bovine serum, 1 μM dexamethasone, 3-isobutyl-1-methylxanthine (0.5 mM), and antibiotics (1% penicillin-streptomycin). Preadipocytes were maintained in this differentiation medium for 3 days and subsequently cultured in adipocyte medium. Cultures were re-fed every 2 to 3 days to allow 90% cells to reach full differentiation before conducting chemical treatment. Chemicals were freshly diluted in adipocyte medium before treatment. Human preadipocytes used in this study were supplied by Zen-Bio (Research Triangle, NC). Preadipocytes were inoculated in DMEM/Ham's F-10 medium (1:1, vol/vol) containing 10% fetal bovine serum, 15 mM HEPES, and antibiotics at a density of 30,000 cells/cm^2. Confluent monolayers of preadipocytes were induced to differentiate with a standard differentiation medium consisting of DMEM-F10 (1:1, vol/vol) medium supplemented with 15 mM HEPES, 3% fetal bovine serum, 33 μM biotin, 17 μM pantothenate, 100 nM insulin, 0.25 μM methylisobutylxanthine, 1 μM dexamethasone, 1 μM BRL49653, and antibiotics. Preadipocytes were maintained in this differentiation medium for 3 days and subsequently cultured in adipocyte medium in which BRL49653 and methylisobutylxanthine were omitted. Cultures were re-fed every 2 to 3 days.

Cells were washed with fresh adipocyte medium, re-fed with medium containing the different treatments, and incubated at 37 °C in 5% CO_2 in air before analysis. Cell viability was measured by trypan blue exclusion.

UCP2 Transfection

UCP2 full-length cDNA was amplified by reverse transcriptase-polymerase chain reaction (RT-PCR) using mRNA isolated from mouse white adipose tissues. The PCR primers for this amplification are shown as follows: UCP2 forward, 5′-GCTAGCATGGTTGGTTTCAAG-3′, reverse, 5′-GCTAGCTCAGAAAGGTGAATC-3′. The PCR products were subcloned into pcDNA4/His expression vectors. The linearized constructs were transfected into 3T3-L1 preadipocytes using lipofectamine plus standard protocol (Invitrogen, Carlsbad, CA). After 48 hours of transfection,

cells were split and cultured in selective medium containing 400 μg/mL zeocin for the selection of resistant colonies. Cells were fed with selective medium every 3 days until resistant colonies could be identified. These resistant foci were picked, expanded, tested for expression, and frozen for future experiments.

Determination of Mitochondrial Membrane Potential

Mitochondrial membrane potential was analyzed fluorometrically with a lipophilic cationic dye JC-1 (5,5′,6,6′-tetrachloro-1,1′,3,3′-tetraethylbenzimidazol carbocyanine iodide) using a mitochondrial potential detection kit (Biocarta, San Diego, CA). Mitochondrial potential was determined as the ratio of red fluorescence (excitation, 550 nm; emission, 600 nm) and green fluorescence (excitation, 485 nm; emission, 535 nm) using a fluorescence microplate reader.

Measurement of $[Ca^{2+}]i$

$[Ca^{2+}]i$ in adipocytes was measured using a fura-2 dual-wavelength fluorescence imaging system. Cells were plated in 35-mm dishes (P35G-0–14-C; MatTek Corp., Ashland, MA). Before $[Ca^{2+}]i$ measurement, cells were put in serum-free medium overnight and rinsed with HEPES balanced salt solution containing the following components (in mM): 138 NaCl, 1.8 $CaCl_2$, 0.8 $MgSO_4$, 0.9 NaH_2PO_4, 4 $NaHCO_3$, 5 glucose, 6 glutamine, 20 HEPES, and 1% bovine serum albumin. Cells were loaded with fura-2 acetoxymethyl ester (10 μM) in the same buffer for 2 hours at 37 °C in a dark incubator with 5% CO_2. To remove extracellular dye, cells were rinsed with HEPES balanced salt solution three times and post-incubated at room temperature for an additional 1 hour for complete hydrolysis of cytoplasmic fura-2 acetoxymethyl ester. The dishes with dye-loaded cells were mounted on the stage of a Nikon S-F fluorescence inverted microscope with a Cohu model 4915 charge-coupled device camera. Fluorescent images were captured alternatively at excitation wavelengths of 340 and 380 nm with an emission wavelength of 520 nm. After establishment of a stable baseline, the responses to $1\alpha,25\text{-}(OH)_2D_3$ was determined. $[Ca^{2+}]i$ was calculated using a ratio equation as described previously. Each analysis evaluated responses of five representative whole cells. Images were analyzed with InCyt Im2 version 4.62 imaging software (Intracellular Imaging, Cincinnati, OH). Images were calibrated using a fura-2 calcium imaging calibration kit (Molecular Probes, Eugene, OR) to create a calibration curve in solution, and cellular calibration was accomplished using digitonin (25 μM) and Tris-EGTA (pH 8.7; 100 mM) to measure maximal and minimal $[Ca^{2+}]i$ levels, respectively.

Total RNA Extraction

A total cellular RNA isolation kit (Ambion, Austin, TX) was used to extract total RNA from cells according to manufacturer's instruction.

Quantitative Real-time PCR

Adipocyte 18s, cyclin A, NADPH oxidase, and UCP2 were quantitatively measured using a Smart Cycler Real-Time PCR System (Cepheid, Sunnyvale, CA) with a TaqMan 1000 Core Reagent Kit (Applied Biosystems, Foster City, CA). The primers and probe sets were ordered from Applied Biosystems TaqMan Assays-on-Demand Gene Expression primers and probe set collection according to the manufacturer's instructions. Pooled adipocyte total RNA was serial-diluted in the range of 1.5625 to 25 ng and used to establish a standard curve; total RNA for unknown samples was also diluted in this range. Reactions of quantitative RT-PCR for standards and unknown samples were also performed according to the instructions of Smart Cycler System (Cepheid) and TaqMan Real Time PCR Core Kit (Applied Biosystems). The mRNA quantitation for each sample was further normalized using the corresponding 18s quantitation.

Assessment of Cell Proliferation

Cells were plated in DMEM with different treatments in duplicate in 96-well plates. After 48 hours, a CyQUANT Cell Proliferation Kit (Molecular Probes) was used following the manufacturer's protocol. A microplate fluorometer (Packard Instrument Co., Downers Grove, IL) was used to measure CyQUANT fluorescence. Cell viability was determined by trypan blue exclusion examination.

Determination of Intracellular ROS Generation

Intracellular ROS generation was assessed using 6-carboxy-2′,7′-dichlorodihydrofluorescein diacetate as described previously (20). Cells were loaded with 6-carboxy-2′,7′-dichlorodihydrofluorescein diacetate (2 μM) 30 minutes before the end of the incubation period (48 hours). After washing twice with phosphate-buffered saline, cells were scraped and disrupted by sonication on ice (20 seconds). Fluorescence (emission, 543 or 527 nm) and DNA content were measured as described previously. The intensity of fluorescence was expressed as arbitrary units per nanogram DNA.

Statistical Analysis

Data were evaluated for statistical significance by one-way or two-way ANOVA, depending on the number of main effect(s) involved, and significantly different group means were separated by the least significant difference test ($p < 0.05$) using SPSS (SPSS, Inc., Chicago, IL). All data are expressed as mean ± standard error (SE).

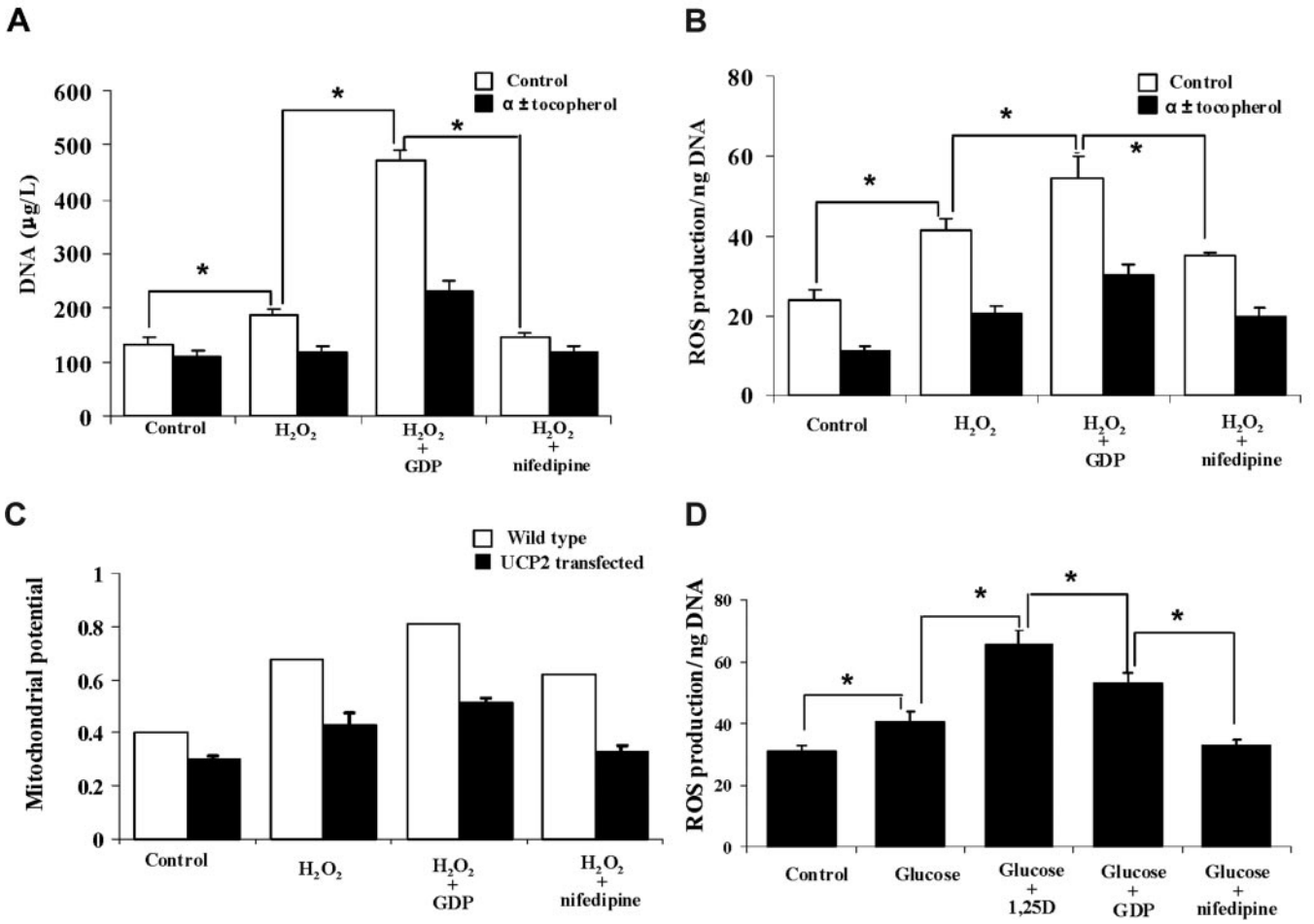

Figure 1: Effects of H_2O_2 on DNA synthesis (A), ROS production (B), and mitochondrial potential (C) and the effect of glucose on ROS production (D) in cultured 3T3-L1 adipocytes. Adipocytes were treated with either H_2O_2 (100 nM) or $\alpha\pm$tocopherol (1 μM), combined with or without GDP (100 μM) or nifedipine (10 μM) for 48 hours. Data are expressed as mean $\pm$ SE ($n = 6$). To test the effect of glucose on ROS production, adipocytes were treated with glucose (30 mM), glucose (30 mM) plus nifedipine (10 μM), glucose (30 mM) plus GDP, or glucose (30 mM) plus 1α,25-$(OH)_2D_3$ (1,25D) for 48 hours. Asterisks above the bars indicate significant differences ($p < 0.05$).

Results

Our first aim was to examine whether ROS exerts an effect on adipocyte proliferation. The data presented in Figure 1A indicate that this is indeed the case. Treatment of 3T3-L1 adipocytes with H_2O_2 increased the total DNA of cultured cells by 39% ($p < 0.001$), whereas addition of antioxidant $\alpha\pm$tocopherol completely blocked this effect. The effect of ROS on adipocyte proliferation seems to be regulated by mitochondrial uncoupling and intracellular calcium homeostasis. Addition of mitochondrial uncoupling inhibitor guanosine 5′-diphosphate (GDP) augmented the stimulation of cell proliferation by H_2O_2 by 183% ($p < 0.005$), whereas the calcium channel antagonist nifedipine had the opposite effect and suppressed H_2O_2 induced cell DNA synthesis ($p < 0.05$). Because inhibiting mitochondrial uncoupling and increasing $[Ca^{2+}]i$ have been shown to contribute to increased ROS production, GDP may increase DNA synthesis by increasing ROS production while nifedpine exerts the opposite effect through suppression of ROS production. Consistent with this, Figure 1B shows that addition of GDP increased ROS production by 30% ($p < 0.01$) compared with H_2O_2 treatment alone, whereas nifedipine reduced H_2O_2-induced ROS production by 25% ($p < 0.003$). Figure 1A and B also show that addition of antioxidant $\alpha\pm$tocopherol inhibited both ROS production and DNA synthesis in all groups. These results suggest that ROS stimulated cell proliferation in cultured adipocytes and that this effect can be regulated by mitochondrial uncoupling status and intracellular homeostasis. Similar results were also observed in human adipocytes (data not shown).

To further study the interaction between ROS and mitochondrial uncoupling status, we measured mitochondrial potential in both wildtype 3T3-L1 adipocytes and UCP2-transfected 3T3-L1 adipocytes. Figure 1C shows that H_2O_2

increased mitochondrial potential by 72% and that addition of GDP augmented this effect ($p < 0.001$), indicating that ROS production inhibits mitochondrial uncoupling. Nifedipine suppressed the H_2O_2 induced increase in mitochondrial potential, and this result confirmed that calcium channel antagonism inhibits ROS production. UCP2 transfection decreased mitochondrial potential ($p < 0.001$) and suppressed the effect of H_2O_2 on mitochondrial uncoupling ($p < 0.001$), indicating that ROS production is regulated, in part, by mitochondrial potential and UCP2.

Figure 1D shows that ROS has a direct role in regulating intracellular calcium homeostasis in 3T3-L1 adipocytes. H_2O_2 induced a 5-fold increase in $[Ca^{2+}]i$ ($p < 0.001$), and this effect was reversed by addition of antioxidant $\alpha\pm$tocopherol. Because suppression of intracellular calcium influx by nifedipine decreased ROS production as described in Figure 1B, this result suggests a positive feedback interaction between ROS production and intracellular calcium homeostasis: ROS stimulates $[Ca^{2+}]i$, and elevated $[Ca^{2+}]i$ also favors ROS production. Similar results were observed in Zen-Bio human adipocytes (data not shown).

Hyperglycemia is one of the most common clinical signs in obesity and diabetes, which have been shown to be associated with increased ROS production. Accordingly, we next studied the effect and mechanism of high glucose level on ROS production and consequent adipocyte proliferation. As shown in Figure 2A, high glucose treatment increased ROS production significantly ($p < 0.05$), and this effect was partially reversed by addition of nifedipine. Addition of GDP further stimulated ROS production compared with glucose alone. Notably, treatment of adipocytes with $1\alpha,25\text{-}(OH)_2D_3$, which was previously found to suppress mitochondrial uncoupling and to increase $[Ca^{2+}]i$ in adipocytes, resulted in greater stimulation of ROS production than either glucose alone or glucose plus GDP ($p < 0.05$), suggesting that $1\alpha,25\text{-}(OH)_2D_3$ stimulates ROS production by both inhibition of mitochondrial uncoupling and stimulation of $[Ca^{2+}]i$. Glucose also increased $[Ca^{2+}]i$ by 3-fold ($p < 0.001$; Figure 2B), and this effect was partially blocked by addition of tocopherol, indicating that stimulation of $[Ca^{2+}]i$ by high glucose is partially attributable to ROS production. Consistent with this, Figure 3A shows that high glucose also increased expression of NADPH oxidase ($p < 0.001$), a key enzyme in ROS production, in both wildtype and UCP2 transfected 3T3-L1 adipocytes, but UCP2 overexpression attenuated this effect. These results suggest that high glucose may increase ROS production by stimulating NADPH oxidase expression. Addition of $1\alpha,25\text{-}(OH)_2D_3$ stimulated NADPH oxidase expression, whereas nifedipine suppressed its expression. Although GDP has been shown to increases ROS production, we found GDP suppressed NADPH oxidase expression, indicating that regulation of ROS production by GDP is not through up-regulation of ROS-generating enzyme gene expression. Figure 3B provides further evidence for the role of UCP2 in the regulation of high glucose–induced ROS production. High glucose inhibits UCP2 expression in both wildtype and UCP2 transfected adipocytes, indicating that high glucose stimulates ROS production by regulating mitochondrial uncoupling status.

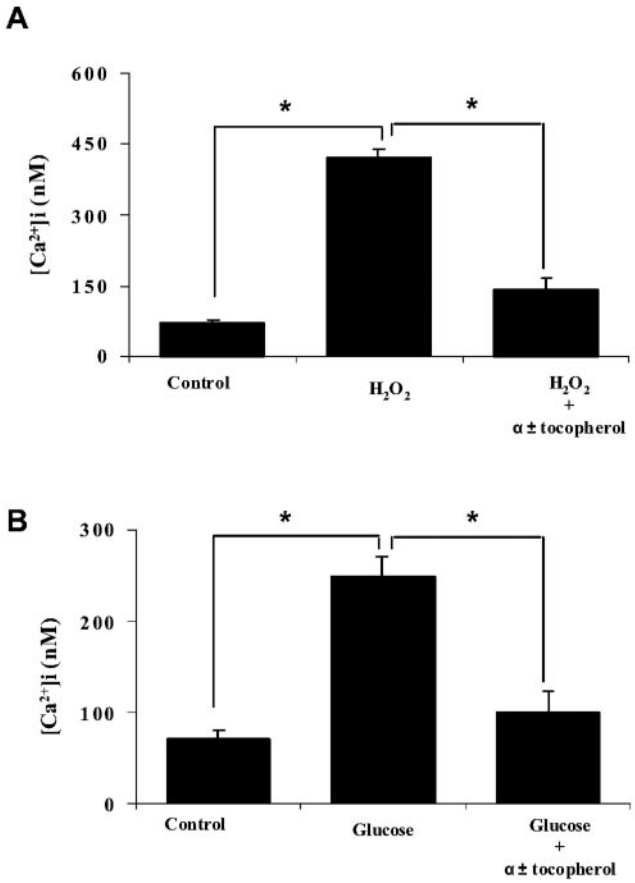

Figure 2: Effects of H_2O_2 (A) and glucose (B) on $[Ca^{2+}]i$ in cultured 3T3-L1 adipocytes. Adipocytes were treated with either H_2O_2 (100 nM) or H_2O_2 (100 nM) plus $\alpha\pm$tocopherol (1 μM) for 4 hours. To test the effect of glucose on ROS production, adipocytes were treated with glucose (30 mM), glucose (30 mM) plus nifedipine (10 μM), glucose (30 mM) plus GDP, or glucose (30 mM) plus $1\alpha,25\text{-}(OH)_2D_3$ (1,25D) for 48 hours. Data are expressed as mean ± SE ($n = 6$). Asterisks above the bars indicate significant differences ($p < 0.05$).

Figure 4A shows that stimulation of ROS production by high glucose is associated with increased DNA synthesis. High glucose alone significantly increased DNA synthesis ($p < 0.03$), and this effect was augmented by addition of GDP or $1\alpha,25\text{-}(OH)_2D_3$. In contrast, inhibition of ROS production by nifedipine decreased glucose induced DNA synthesis ($p < 0.05$). To further study the effect of high glucose on adipocyte proliferation, we also observed the expression of cyclin A (Figure 4B). Consistent with the DNA synthesis data, high glucose stimulated cyclin A ex-

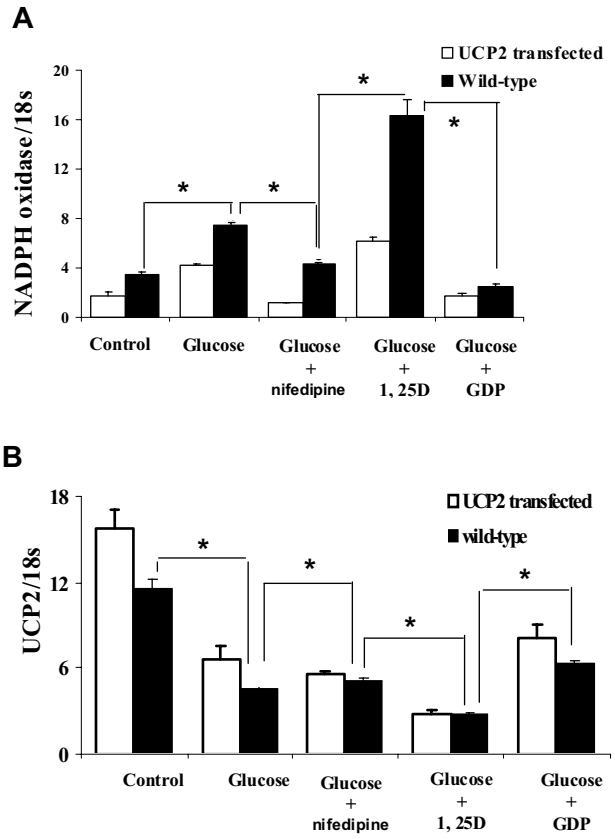

Figure 3: Effects of glucose on the expression of NADPH oxidase (A) and UCP2 (B) in cultured 3T3-L1 adipocytes. Adipocytes were treated with glucose (30 mM), glucose (30 mM) plus nifedipine (10 μM), glucose (30 mM) plus GDP, or glucose (30 mM) plus 1,25-$(OH)_2D_3$ for 48 hours. Values are normalized to 18s expression, and data are expressed as mean ± SE (n = 6). Asterisks above the bars indicate significant differences ($p < 0.05$).

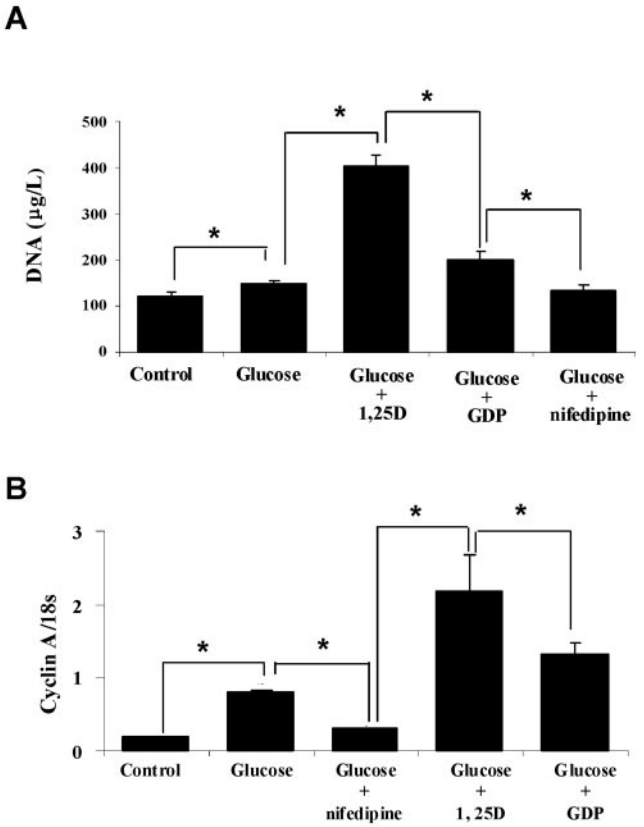

Figure 4: Effects of glucose on DNA synthesis (A) and the expression ratio of cyclin A (B) in cultured 3T3-L1 adipocytes. Adipocytes were treated with glucose (30 mM), glucose (30 mM) plus nifedipine (10 μM), glucose (30 mM) plus GDP, or glucose (30 mM) plus 1α,25-$(OH)_2D_3$ for 48 hours. Data are expressed as mean ± SE (n = 6). Asterisks above the bars indicate significant differences ($p < 0.05$).

pression by 3-fold ($p < 0.001$), and GDP and 1α,25-$(OH)_2D_3$ augmented this effect, whereas nifedipine suppressed it. These data suggest high glucose stimulates adipocyte proliferation, and this effect may be at least partially mediated by its stimulation of ROS production.

Discussion

Obesity and diabetes are associated with increased oxidative stress, and ROS may play a role in regulation of adipocyte proliferation. In this study, we showed that a low concentration of H_2O_2 stimulates cell proliferation in cultured adipocytes. This effect can be augmented by a mitochondrial uncoupling inhibitor and suppressed by a calcium channel antagonist, indicating that mitochondrial potential and intracellular calcium homeostasis may play a role in regulation of ROS-induced cell proliferation. 1α,25-$(OH)_2D_3$, which has been shown to stimulate $[Ca^{2+}]i$ and to inhibit UCP2 expression, stimulates ROS production and cell proliferation in adipocytes. High glucose also exerts stimulatory effect on ROS production, and this effect can be augmented by addition of 1α,25-$(OH)_2D_3$, suggesting that 1α,25-$(OH)_2D_3$ may be involved in the regulation of ROS production in adipocytes. These results indicate that strategies to suppress 1α,25-$(OH)_2D_3$ levels, such as increasing dietary calcium, may reduce oxidative stress and thereby inhibit ROS-induced stimulation of adipocyte proliferation. Indeed, we recently showed that increasing dietary calcium attenuates adipose tissue ROS production in aP2-*agouti* transgenic mice fed a high-sucrose/high-fat diet (38).

Increased oxidative stress has been reported in both humans and animal models of obesity (12,13), suggesting that ROS may play a critical role in the mechanisms underlying proliferative responses. This concept is supported by evidence that both H_2O_2 and superoxide anion induce mitogenesis and cell proliferation in several mammalian cell

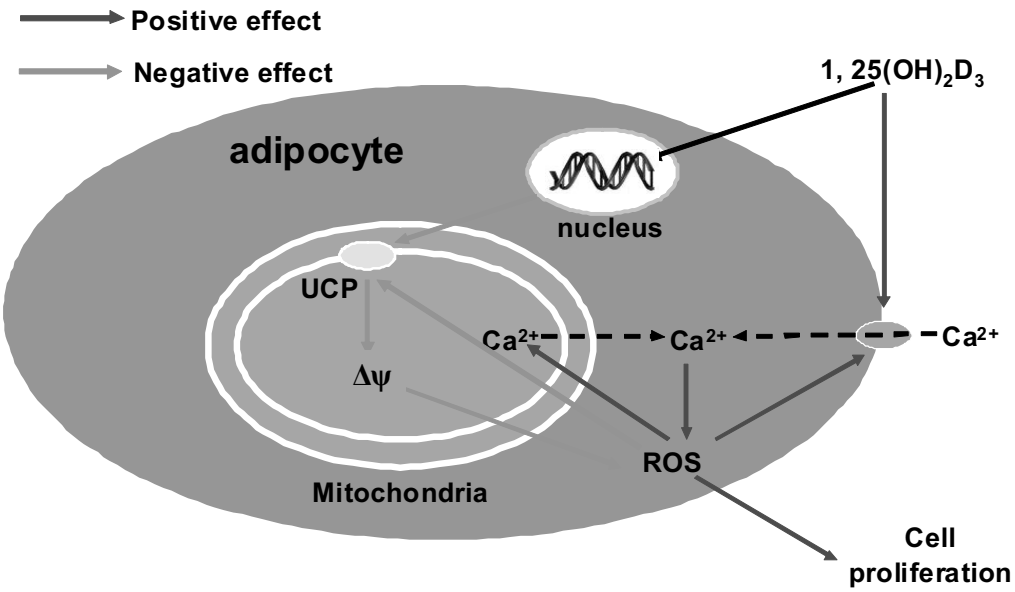

Figure 5: Schematic illustration of effects and mechanisms of 1α,25-$(OH)_2D_3$ on ROS production and adipocyte proliferation. Physiologic doses of 1α,25-$(OH)_2D_3$ increase ROS production by inhibiting UCP2 expression and stimulating intracellular calcium influx, resulting in a consequent increase in adipocyte proliferation.

types (22). Furthermore, reduction of oxidants through supplementation with antioxidants inhibits cell proliferation in vitro (39,40). Although the mechanisms for the involvement of oxidative stress in the induction of cell proliferation are not known, it has been shown that ROS and other free radicals influence the expression of number of genes and transduction pathways involved in cell growth and proliferation. The most significant effects of oxidants on signaling pathways have been observed in the mitogen-activated protein kinase/activatory protein-1, and it has been suggested that ROS can activate mitogen-activated protein kinases and thereby transcription factor activator protein-1 (41), a collection of dimeric basic region-leucine zipper proteins that activate cyclin-dependent kinase and entry into cell division cycle (42). Furthermore, the elevation of cytosolic calcium level induced by ROS results in activation of protein kinase C required for expression of positive regulators of cell proliferation such as c-fos and c-jun (43–45). ROSs have also been implicated as a second messenger involved in activation of nuclear factor-κB (NF-κB) (46), whose expression has been shown to stimulate cell proliferation through tumor necrosis factor and interleukin-1 (47). The effect of ROS on NF-κB activation is further supported by studies that showed that expression of NF-κB can be suppressed by antioxidants (48,49). In addition, ROS can modify DNA methylation and cause oxidative DNA damage, which results in decreased methylation patterns (50), and consequently, contributes to an overall aberrant gene expression. ROS may also attribute to the inhibition of cell-to-cell communication, and this effect can result in decreased regulation of homeostatic growth control of normal surrounding cells and lead to clonal expansion (51,52). Despite these mechanisms proposed to explain the stimulatory effect on cell proliferation, limited studies have been conducted on adipocytes. In this study, we showed that low concentrations of ROS promote cell proliferation in cultured human and murine adipocytes. However, further study for the underlying molecular mechanisms is needed.

The yield of ROS can be efficiently modulated by mitochondrial uncoupling. Korshunov et al. (53) have shown that slight increase of the H^+ backflux (to the matrix), which diminishes $\Delta\psi$, results in a substantial decrease of mitochondrial ROS formation. Accordingly, the H^+ backflow from UCP-induced uncoupling would be expected to down-regulate ROS production. In addition, calcium can active ROS-generating enzymes directly, and activation of calcium-dependent protein kinase C favors assembly of the active NADPH oxidase complex (31), indicating that $[Ca^{2+}]i$ may be another key player in regulation of ROS production. Accordingly, it is reasonable to propose that 1α,25-$(OH)_2D_3$, which has been shown to inhibit mitochondrial uncoupling genomically (37) and to stimulate $[Ca^{2+}]i$ through a membrane receptor for 1,25$(OH)_2D_3$ (36,54,55) in adipocytes, would stimulate ROS production and may consequently be involved in the regulation of adipocyte proliferation. Indeed, in this study, we showed that addition of 1α,25-$(OH)_2D_3$ augmented high glucose-induced ROS production and adipocyte proliferation. This effect was further enhanced by a mitochondrial uncoupling inhibitor and suppressed by calcium channel antagonism, indicating that

1α,25-$(OH)_2D_3$ stimulates ROS production by increasing $[Ca^{2+}]i$ and by inhibiting mitochondrial uncoupling. Furthermore, previous studies have suggested that 1α,25-$(OH)_2D_3$ may act as an pro-oxidant in various cell types (56) and that treatment with 1α,25-$(OH)_2D_3$ inhibited the expression of the major constituents of the cellular defense system against ROS (57).

Previous data from our laboratory have shown that 1α,25-$(OH)_2$-D_3 seems to modulate adipocyte lipid and energy metabolism through both genomic and non-genomic pathways (35–37). We have reported that 1α,25-$(OH)_2$-D_3 plays a direct role in the modulation of adipocyte Ca^{2+} signaling, resulting in an increased lipogenesis and decreased lipolysis (36). In addition, 1α,25-$(OH)_2D_3$ also plays a role in regulating human adipocyte UCP2 mRNA and protein levels, indicating that the suppression of 1α,25-$(OH)_2D_3$ and the resulting up-regulation of UCP2 may contribute to increased rates of lipid oxidation (37). In addition, we also showed that physiologic doses of 1α,25-$(OH)_2D_3$ inhibit apoptosis in differentiated human and 3T3-L1 adipocytes (4) and that the suppression of 1α,25-$(OH)_2D_3$ in vivo by increasing dietary calcium stimulates adipocyte apoptosis in aP2 transgenic mice (58), suggesting that the stimulation of adipocyte apoptosis contributes to the observed reduction in adipose tissue mass after administration of high-calcium diets (37). Accordingly, the suppression of 1α,25-$(OH)_2D_3$ by increasing dietary calcium attenuates adipocyte triglyceride accumulation and caused a net reduction in fat mass in both mice and humans in the absence of caloric restriction (59,60), a marked augmentation of body weight and fat loss during energy restriction in both mice and humans (59–62), and a reduction in the rate of weight and fat regain after energy restriction in mice (58). Data from this study provided further evidence to support the role of 1α,25-$(OH)_2D_3$ in favoring energy storage and fat mass expansion by stimulating ROS production and adipocyte proliferation. As shown in Figure 5, ROS stimulates adipocyte proliferation, and this effect can by suppressed by mitochondrial uncoupling and stimulated by elevation of $[Ca^{2+}]i$. 1α,25-$(OH)_2D_3$ increases ROS production by inhibiting UCP2 expression and increasing $[Ca^{2+}]i$, consequently favoring adipocyte proliferation. Accordingly, these data suggest that suppression 1α,25-$(OH)_2D_3$ by increasing dietary calcium may reduce 1α,25-$(OH)_2D_3$–mediated ROS production and limit ROS-induced adipocyte proliferation, potentially resulting in reduced adiposity.

The data presented here show a direct effect of oxidative stress on adipocyte proliferation in white adipose tissue, and this observation may have important implications in understanding the adipose mass changes observed under oxidative stress. However, cell proliferation was only evaluated by DNA content and cyclin expression level. Furthermore, various sources of ROS production may play different roles in regulation of cell signaling in cell cycle and cell metabolism. Although we showed that both mitochondrial ROS production and cellular enzymatic ROS production are associated with adipocyte proliferation, the contribution of each source needs further study.

Acknowledgments

This study was supported, in part, by the Tennessee Agricultural Experiment Station.

References

1. **Bonnet FP.** Fat cell size and number in obese children. *Adipose Tissue Childhood.* 1981;17:133–54.
2. **Brook CG, Lloyd JK, Wolf OH.** Relation between age of onset of obesity and size and number of adipose cells. *Br Med J.* 1972;2:25–7.
3. **Reuter W, Ulbricht W.** Adipocyte volume and count in obesity during weight reduction. *Z Gesamte Inn Med.* 1987; 42:372–3.
4. **Sun X, Zemel MB.** Role of uncoupling protein 2 (UCP2) expression and 1alpha, 25-dihydroxyvitamin D3 in modulating adipocyte apoptosis. *FASEB J.* 2004;18:1430–2.
5. **Hargrave KM, Meyer BJ, Li C, Azain MJ, Baile CA, Miner JL.** Influence of dietary conjugated linoleic acid and fat source on body fat and apoptosis in mice. *Obes Res.* 2004;12:1435–44.
6. **Gullicksen PS, Della-Fera MA, Baile CA.** Leptin-induced adipose apoptosis: implications for body weight regulation. *Apoptosis.* 2003;8:327–35.
7. **Unger RH.** Minireview: weapons of lean body mass destruction: the role of ectopic lipids in the metabolic syndrome. *Endocrinology.* 2003;144:5159–65.
8. **Raz I, Eldor R, Cernea S, Shafrir E.** Diabetes: insulin resistance and derangements in lipid metabolism. Cure through intervention in fat transport and storage. *Diabetes Metab Res Rev.* 2005;21:3–14.
9. **Andersen O, Haugaard SB, Andersen UB, et al.** Lipodystrophy in human immunodeficiency virus patients impairs insulin action and induces defects in beta-cell function. *Metabolism.* 2003;52:1343–53.
10. **El-Haschimi K, Dufresne SD, Hirshman MF, Flier JS, Goodyear LJ, Bjorbaek C.** Insulin resistance and lipodystrophy in mice lacking ribosomal S6 kinase 2. *Diabetes.* 2003;52:1340–6.
11. **Yang X, Jansson PA, Nagaev I, et al.** Evidence of impaired adipogenesis in insulin resistance. *Biochem Biophys Res Commun.* 2004;317:1045–51.
12. **Sonta T, Inoguchi T, Tsubouchi H, et al.** Evidence for contribution of vascular NAD(P)H oxidase to increased oxidative stress in animal models of diabetes and obesity. *Free Radic Biol Med.* 2004;37:115–23.
13. **Atabek ME, Vatansev H, Erkul I.** Oxidative stress in childhood obesity. *J Pediatr Endocrinol Metab.* 2004;17:1063–8.
14. **Inoguchi T, Li P, Umeda F, et al.** High glucose level and free fatty acid stimulate reactive oxygen species production through protein kinase C–dependent activation of NAD(P)H oxidase in cultured vascular cells. *Diabetes.* 2000;49:1939–45.

15. **Shangari N, O'Brien PJ.** The cytotoxic mechanism of glyoxal involves oxidative stress. *Biochem Pharmacol.* 2004; 68:1433–42.
16. **Chung SS, Ho EC, Lam KS, Chung SK.** Contribution of polyol pathway to diabetes-induced oxidative stress. *J Am Soc Nephrol.* 2003;14:S233–6.
17. **Inoguchi T, Sonta T, Tsubouchi H, et al.** Protein kinase C-dependent increase in reactive oxygen species (ROS) production in vascular tissues of diabetes: role of vascular NAD(P)H oxidase. *J Am Soc Nephrol.* 2003;14:S227–32.
18. **Talior I, Tennenbaum T, Kuroki T, Eldar-Finkelman H.** Protein kinase C-{delta} dependent activation of oxidative stress in adipocytes of obese and insulin resistant mice: role for NADPH oxidase. *Am J Physiol Endocrinol Metab.* 2005; 288:E405–11.
19. **Fiordaliso F, Bianchi R, Staszewsky L, et al.** Antioxidant treatment attenuates hyperglycemia-induced cardiomyocyte death in rats. *J Mol Cell Cardiol.* 2004;37:959–68.
20. **Manea A, Constantinescu E, Popov D, Raicu M.** Changes in oxidative balance in rat pericytes exposed to diabetic conditions. *J Cell Mol Med.* 2004;8:117–26.
21. **Mishra KP.** Cell membrane oxidative damage induced by gamma-radiation and apoptotic sensitivity. *J Environ Pathol Toxicol Oncol.* 2004;23:61–6.
22. **Burdon RH.** Superoxide and hydrogen peroxide in relation to mammalian cell proliferation. *Free Radic Biol Med.* 1995;18: 775–94.
23. **Burdon RH, Gill V, Rice-Evans C.** Oxidative stress and tumour cell proliferation. *Free Radic Res.* 1990;11:65–76.
24. **Murrell GAC, Francis MJO, Bromley L.** Modulation of fibroblast proliferation by oxygen free radicals. *Biochem J.* 1990;265:659–65.
25. **Crawford D, Zbinden I, Amstad P, Cerutti P.** Oxidant stress induces the protooncogenes *c-fos* and *c-myc* in mouse epidermal cells. *Oncogene.* 1989;3:27–32.
26. **Shibanuma M, Kuroki T, Nose M.** Induction of DNA replication and expression of protooncogenes *c-myc* and *c-fos* in quiescent Balb/3T3 cells by xanthine-xanthine oxidase. *Oncogene.* 1988;3:17–21.
27. **Nose K, Shibanuma M, Kikuchi K, Kazeyana H, Sakiyama S, Kuroki T.** Transcriptional activities of early response genes in a mouse osteoblastic cell line. *Eur J Biochem.* 1991;201: 99–106.
28. **Amstad PA, Krupitza G, Cerutti P.** Mechanism of *c-fos* induction by active oxygen. *Cancer Res.* 1992;52:3952–60.
29. **Daou GB, Srivastava AK.** Reactive oxygen species mediate endothelin-1-induced activation of ERK1/2, PKB, and Pyk2 signaling, as well as protein synthesis, in vascular smooth muscle cells. *Free Radic Biol Med.* 2004;37:208–15.
30. **Mohamed AK, Bierhaus A, Schiekofer S, Tritschler H, Ziegler R, Nawroth PP.** The role of oxidative stress and NF-kappaB activation in late diabetic complications. *Biofactors.* 1999;10:157–67.
31. **Gordeeva AV, Zvyagilskaya RA, Labas YA.** Cross-talk between reactive oxygen species and calcium in living cells. *Biochemistry (Mosc).* 2003;68:1077–80.
32. **Volk T, Hensel M, Kox WJ.** Transient Ca2+ changes in endothelial cells induced by low doses of reactive oxygen species: role of hydrogen peroxide. *Mol Cell Biochem.* 1997; 171:11–21.
33. **Casteilla L, Rigoulet M, Penicaud L.** Mitochondrial ROS metabolism: modulation by uncoupling proteins. *IUBMB Life.* 2001;52:181–8.
34. **Miwa S, Brand MD.** Mitochondrial matrix reactive oxygen species production is very sensitive to mild uncoupling. *Biochem Soc Trans.* 2003;31:1300–1.
35. **Zemel MB.** Role of calcium and dairy products in energy partitioning and weight management. *Am J Clin Nutr.* 2004; 79:907S–12S.
36. **Shi H, Norman AW, Okamura WH, Sen A, Zemel MB.** 1alpha,25-Dihydroxyvitamin D3 modulates human adipocyte metabolism via nongenomic action. *FASEB J.* 2001;15: 2751–3.
37. **Shi H, Norman AW, Okamura WH, Sen A, Zemel MB.** 1alpha,25-dihydroxyvitamin D3 inhibits uncoupling protein 2 expression in human adipocytes. *FASEB J.* 2002;16:1808–10.
38. **Sun XC, Zemel MB.** Dietary calcium regulates ROS production in aP2-agouti transgenic mice on high fat/high sucrose diets. *Int J Obes Relat Metab Disord.* 2006;30:1341–6.
39. **Khan N, Sultana S.** Induction of renal oxidative stress and cell proliferation response by ferric nitrilotriacetate (Fe-NTA): diminution by soy isoflavones. *Chem Biol Interact.* 2004;149: 23–35.
40. **Simeone AM, Tari AM.** How retinoids regulate breast cancer cell proliferation and apoptosis. *Cell Mol Life Sci.* 2004;61: 1475–84.
41. **Chang L, Karin M.** Mammalian MAP kinase signalling cascades. *Nature.* 2001;410:37–40.
42. **Kouzarides T, Ziff E.** Leucine zippers of fos, jun and GCN4 dictate dimerization specificity and thereby control DNA binding. *Nature.* 1989;340:568–71.
43. **Lin JK.** Suppression of protein kinase C and nuclear oncogene expression as possible action mechanisms of cancer chemoprevention by Curcumin. *Arch Pharm Res.* 2004;27: 683–92.
44. **Athar M.** Oxidative stress and experimental carcinogenesis. *Indian J Exp Biol.* 2002;40:656–67.
45. **Hollander MC, Fornace AJ Jr.** Induction of fos RNA by DNA-damaging agents. *Cancer Res.* 1989;49:1687–92.
46. **Song YS, Rosenfeld ME.** Methionine-induced hyperhomocysteinemia promotes superoxide anion generation and NFkappaB activation in peritoneal macrophages of C57BL/6 mice. *J Med Food.* 2004;7:229–34.
47. **Giri DK, Aggarwal BB.** Constitutive activation of NF-kappaB causes resistance to apoptosis in human cutaneous T cell lymphoma HuT-78 cells. Autocrine role of tumor necrosis factor and reactive oxygen intermediates. *J Biol Chem.* 1998; 273:14008–14.
48. **Nomura M, Ma W, Chen N, Bode AM, Dong Z.** Inhibition of 12-O-tetradecanoylphorbol-13-acetate-induced NF-kappaB activation by tea polyphenols, (-)-epigallocatechin gallate and theaflavins. *Carcinogenesis.* 2000;21:1885–90.
49. **Schulze-Osthoff K, Bauer MK, Vogt M, Wesselborg S.** Oxidative stress and signal transduction. *Int J Vitam Nutr Res.* 1997;67:336–42.

50. **Weitzman SA, Turk PW, Milkowski DH, Kozlowski K.** Free radical adducts induce alterations in DNA cytosine methylation. *Proc Natl Acad Sci U S A.* 1994;91:1261–4.
51. **Cerutti P, Ghosh R, Oya Y, Amstad P.** The role of the cellular antioxidant defense in oxidant carcinogenesis. *Environ Health Perspect.* 1994;102:123–9.
52. **Upham BL, Kang KS, Cho HY, Trosko JE.** Hydrogen peroxide inhibits gap junctional intercellular communication in glutathione sufficient but not glutathione deficient cells. *Carcinogenesis.* 1997;18:37–42.
53. **Korshunov SS, Skulachev VP, Starkov AA.** High protonic potential actuates a mechanism of production of reactive oxygen species in mitochondria. *FEBS Lett.* 1997;416:15–8.
54. **Nemere I, Safford SE, Rohe B, DeSouza MM, Farach-Carson MC.** Identification and characterization of 1,25D3-membrane-associated rapid response, steroid (1,25D3-MARRS) binding protein. *J Steroid Biochem Mol Biol*. 2004; 89–90:281–5.
55. **Fleet JC.** Rapid, membrane-initiated actions of 1,25 dihydroxyvitamin D: what are they and what do they mean. *J Nutr.* 2004;134:3215–8.
56. **Koren R, Hadari-Naor I, Zuck E, Rotem C, Liberman UA, Ravid A.** Vitamin D is a prooxidant in breast cancer cells. *Cancer Res.* 2001;61:1439–44.
57. **Banakar MC, Paramasivan SK, Chattopadhyay MB, et al.** 1alpha, 25-dihydroxyvitamin D3 prevents DNA damage and restores antioxidant enzymes in rat hepatocarcinogenesis induced by diethylnitrosamine and promoted by phenobarbital. *World J Gastroenterol.* 2004;10:1268–75.
58. **Sun X, Zemel MB.** Calcium and dairy products inhibit weight and fat regain during ad libitum consumption following energy restriction in Ap2-Agouti transgenic mice. *J Nutr.* 2004; 134:3054–60.
59. **Zemel MB, Thompson W, Milstead A, Morris K, Campbell P.** Calcium and dairy acceleration of weight and fat loss during energy restriction in obese adults. *Obes Res.* 2004;12: 582–90.
60. **Zemel MB, Shi H, Greer B, Dirienzo D, Zemel PC.** Regulation of adiposity by dietary calcium. *FASEB J.* 2000;14: 1132–8.
61. **Zemel MB, Richards J, Milstead A, Campbell P.** Effects of calcium and dairy on body composition and weight loss in African-American adults. *Obes Res.* 2005;13:1218–25.
62. **Zemel MB, Richards J, Mathis S, Milstead A, Gebhardt L, Silva E.** Dairy augmentation of total and central fat loss in obese subjects. *Int J Obes (Lond).* 2005;29:391–7.